Research Article

Comparative Adsorption of Ibuprofen and Ciprofloxacin from Aqueous Solution Using Natural Bentonite Clay: Experimental and DFT Study

K. E. Onwuka[1,*], A. A. Ahuchaogu[2], O. C. Atasie[3], V. C. Oguike[4], A. C. Nwosu[5], N.B Nwosu[2], J. O. Nwagba[2]

[1]Chemistry Research Unit, Department of Science Laboratory Technology, Federal Polytechnic, Ngodo-Isuochi, Abia State, Nigeria
[2]Department of Pure and Industrial Chemistry, Abia State University Uturu, Abia State, Nigeria. P.M.B. 2000
[3]Department of Biochemistry, Abia State University Uturu, Abia State, Nigeria. P.M.B. 2000
[4]Biology Research Unit, Department of Science Laboratory Technology, Imo State Polytechnic, Omuma, Imo State, Nigeria
[5]Department of Biochemistry, Michael Okpara University Of Agriculture, Umudike, Abia State, Nigeria
*e-mail: ke.onwuka@fpi.edu.ng

Abstract: This study examines the adsorption characteristics of ibuprofen (IBP) and ciprofloxacin (CIP) onto bentonite (BT) in aqueous medium. To investigate surface properties, SEM, FTIR and XRD techniques were used to characterize the bentonite applied as adsorbent. The results confirmed the properties of typical bentonite clay as acceptable. Batch adsorption studies were conducted under different adsorption experimental conditions. The outcome indicated that pH, initial IBP/CIP concentration, adsorbent dosage, contact time and temperature greatly influenced IBP/CIP removal by BT in aqueous medium. Adsorption equilibrium was attained after 240 minutes of contact time for both IBP and CIP with a percentage removal of 87.7% and 59.5% respectively. The pseudo first order, pseudo second order, and intraparticle diffusion kinetic models were utilized to describe the kinetic data, while the Langmuir, Freundlich, and Temkin isotherm models were fitted to the equilibrium data. Results obtained from kinetic and isotherm studies showed that both the kinetic and equilibrium data were efficiently described by the pseudo second order kinetic model and Freundlich isotherm model for both pharmaceuticals respectively, as evidenced by correlation coefficients (R^2) exceeding 0.98 and lower chi-square (χ^2) values observed. Comparatively, thermodynamic analysis indicated that the removal of IBP/CIP from aqueous solution by BT is spontaneous, endothermic, and characterized by increased disorder. Analysis from density functional theory (DFT) was incorporated into experimental findings in other to gain clarity on distinctive characteristics of IBP/CIP adsorption. CIP (4.19 eV) was found to be more reactive than IBP (5.88 eV), due to a lower HOMO-LUMO energy gap (ΔH-L). Generally, greater chemical molecular reactivity, lower water solubility, decreased steric hindrance effects, as well as greater hydrophobicity, were factors mostly responsible for the improved ibuprofen and ciprofloxacin adsorption by bentonite.

Keywords: thermodynamics; ibuprofen; ciprofloxacin; isotherm; kinetics; bentonite

I. INTRODUCTION

Water is an essential resource that humans and other living things can easily access to maintain life, yet industrial and anthropogenic activities has resulted to persistent water pollution. Most of these contaminants—which include pesticides, heavy metals, plastics, hydrocarbons, dyes, paint, and pigments—endanger the health of living things by contaminating surface and underground water.

Researchers have recently started to focus on emerging contaminants (another category of pollutants), such as pharmaceuticals, flame retardants, endocrine disruptors and artificial sweeteners, among others, just to mention very few [1, 2]. Emerging contaminants (ECs) continue to enter the marine environment through both treated and untreated water, leading to pollution [3]. Because emerging contaminants were not considered during design of wastewater treatment plants, however, they are not entirely eliminated

from the plants. This results to frequent aquatic environmental pollution by emerging contaminants, which causes bioaccumulation, negatively affecting both living things and the environment as a whole [4].

The risk of continuously exposing aquatic life to emerging pollutants extends beyond their apparent acute toxicity; aquatic life may become resistant to infections, which could lead to endocrine disruption [5]. Because of these observed negative health effects linked to emerging pollutants, their increased environmental presence has become a major global problem seeking immediate attention [4]. Frequently, Active non-steroidal anti-inflammatory drug (NSAID), mostly, ibuprofen (IBP) has been identified in both underground and surface water at concentrations higher than 1µg/L [6]. Its accumulated presence in the environment becomes a worry due to its high availability and consumption, as well as the restricted ability of traditional wastewater treatment plants to fully treat it during wastewater treatment [7]. Conversely, ciprofloxacin (CIP) is a broad-spectrum antibiotic used to treat a variety of infections caused by gram-negative bacteria, including gastrointestinal, skin, and bone infections, respiratory tract infections, and sexually transmitted infections [8]. Some of these infections are sometimes introduced mechanically into our surrounding directly or indirectly via architectural designs and urban planning [9]. CIP shares a structure with nalidixic acid and is derived from quinolones [10]. It can be taken orally or intravenously, and following oral intake, it has a bioavailability of roughly 70–80%, which spreads throughout bodily fluids and tissues [8]. Within 3 to 5 hours, 20 to 35% of the unmetabolized ciprofloxacin is eliminated as faeces, and 40 to 50% of the drug is left unmetabolized in the system and eliminated as urine [9]. These previously mentioned emerging contaminants end up in the ecosystem, causing issues that are extremely concerning for the environment.

Although, CIP and IBP are both commonly used pharmaceuticals that frequently appear in wastewater, raising significant concerns regarding their potential impacts on human health and the environment, CIP is primarily utilized for treating bacterial infections, while IBP serves as a pain reliever. The distinct structural characteristics of these two drugs present an opportunity to investigate how these differences influence their adsorption onto materials like clay. CIP's more intricate structure, featuring multiple functional groups, may interact with clay in ways that differ from the simpler structure of IBP. This variation can result in differing adsorption capacities and mechanisms, which are essential for formulating effective strategies for wastewater treatment.

Pharmaceuticals in aqueous media have been mitigated by applying various methods, including but not limited to: photodegradation [11], coagulation-flocculation and chlorination [12], biodegradation [13], and advanced oxidation processes (AOPs) [14]. Nevertheless, the majority of these methods are costly and constrained by their poor effectiveness and detrimental effects on the environment [15]. As a matter of fact, it is pertinent to consider other alternative techniques to enable cover up this gap. For this purpose, adsorption technology can be very suitable, since it exhibits the potential of overcoming the drawbacks associated with other aforementioned techniques [15]. Numerous adsorbents have been studied for the purpose of sorbing emerging contaminants like pharmaceuticals. For industrial suitability, acceptability and applicability, an adsorbent must be less toxic (eco-friendly), cheap and readily available. In addition, natural clay and clay-based materials exhibit some reasonable level of porosity and display unique geometries, although sometimes may be incredibly elaborate [16]; they are in compliance with most of these criteria and hence, they have found wide application as suitable adsorbents for the mitigation of numerous organic and inorganic pollutants from aqueous systems.

Owing to their significant hydration potential for inorganic cations found in their interlayer spacings, bentonites (BT) are highly expandable clay minerals that exhibit hydrophobicity [6]. Using quaternary alkyl ammonium cations (QACs) to organophilize clays through the cation exchange mechanism may make them ideal for hydrophobic sorption [6]. Both cationic and anionic surfactants have been used as clay modifiers in many studies to remove organic contaminants from water [17]. Despite their apparent effectiveness, these modification techniques are expensive, only suitable for small-scale applications, and may eventually lose their usefulness for larger-scale ones [1]. Clays are widely accessible in Nigeria and other West African nations, and the ceramics industry frequently uses them to produce goods based on ceramics. They can, however, be used successfully for different purposes. Materials made of clay have been effectively employed to reduce environmental micropollutants [1, 18–20].

Since information about distinctive molecular chemical reactivity and electronic structures of molecules can be helpful in understanding their individual adsorption mechanisms, many researchers have recently explored the use of quantum chemical molecular descriptors for further elucidation of adsorption mechanisms [21]. Any organic compound's chemical reactivity can be determined by DFT calculations [22]. Quantum chemical descriptors, mostly E_L LUMO- lowest unoccupied molecular orbital energy and E_H HOMO- highest occupied molecular orbital energy

were being used in this investigation to glean insight into the complete mechanism underlying the entire adsorption process.

This study investigates the use of bentonite clay as an effective sorbent for the removal of IBP and CIP from simulated pharmaceutical wastewater. The research focuses on various experimental conditions, including temperature, initial drug concentration, adsorbent dosage, contact time, and pH, to assess their impact on drug adsorption behaviour. Kinetic and equilibrium studies are conducted to elucidate the underlying adsorption mechanisms, while density functional theory calculations are employed to provide insights into the molecular interactions between the drugs and the BT. The findings aim to enhance the understanding of BT's potential in wastewater treatment applications, particularly for pharmaceutical contaminants.

II. Experimental

1. Preparation of adsorbent

In this research, BT utilized as an adsorbent was obtained from Umuahia North Local Government area of Abia State, Nigeria. BT beneficiation processes for this study have been fully described in our previous work [23] Approximately 30 grams of BT was subjected to agitation in 1000 mL of deionized water utilizing a mechanical stirrer at 600 rpm for 24 hours at 28 ± 2 °C to enable swelling, and the mixture was further centrifuged at 600 rpm for 15 minutes to eradicate precipitated impurities. According to Amare and Tompai, [24], the presence of moisture in soil and clay particles can influence their structural properties. Therefore, purified BT was then dried in an oven at a temperature of 110 °C for a period of 24 hours and the dried caked clay was further crushed and fine particles sieved through a 125 μm mesh sieve [23]. The Sear's procedure [23] was applied in other to determine the surface area of BT, which was found as 327 m^2/g, and the cation exchange capacity (CEC) was also ascertained as 30.94 meq/100g by utilizing the ammonium acetate procedure [25]. Afterward, the adsorbent was preserved in a desiccator for further use.

2. Adsorbent characterization by surface analytical methods

X-ray diffraction (XRD), scanning electron microscopy (SEM), and Fourier transform infrared spectroscopy (FTIR) were used to characterize the adsorbent. A brief description of these techniques as contained in our previously published work [23], are presented below:

The composition of the adsorbent was analyzed using a Bruker D8 ADVANCE X-ray diffractometer from Germany. A sample of 20 mg of the adsorbent was ultrasonically dispersed in 1 mL of 95% ethanol and then dried as oriented aggregates on separate circular glass slides with a diameter of 2.5 cm. Additionally, 20 mg of BT was dispersed in 1 mL of water and dried on glass slides. The basal X-ray diffraction spacing was recorded using Ni-filtered Cu Kα radiation (1.5406 Å) with a diffractometer equipped with a graphite monochromator, a solid-state detector, and an autosampler. Digital intensity and 2θ values from scans ranging from 2° to 20° were recorded on disk and subsequently processed with a graphics program to generate X-ray diffraction patterns.

Surface topographical data were acquired through a morphological analysis conducted with a Scanning Electron Microscope (SEM) model AIS-2100 from Seron Technologies, South Korea. The adsorbent sample was affixed to a stub using a graphite conductive adhesive paste and then securely mounted on a cylindrical rod that acts as the sample holder. This rod was subsequently inserted into the SEM's analysis chamber, which maintained a vacuum throughout the analysis. When the primary electron beam from the light source interacts with the sample, it causes the emission of various secondary electrons from the surface, each unique to the specific sample. These emitted electrons are captured by different secondary electron detectors, and the resulting signals are utilized to create images of the specimen.

The variations in the functional groups of the adsorbent was analyzed using the Buck Scientific M530 FTIR instrument (USA). This device consists of a deuterated triglycinesulfate detector and a potassium bromide beam splitter, with spectra obtained and processed using Gram A1 software. Approximately 1.0 g of the adsorbent was placed on a salt pellet, and FTIR spectra were recorded in the frequency range of 4,000 to 400 cm^{-1}, with 32 scans at a resolution of 4 cm^{-1}, with results presented as transmittance values.

3. Preparation and physicochemical properties of the target adsorbates

The emerging pharmaceutical contaminants: IBP (purity ≥99%) – a product of Sigma Aldrich (Switzerland) and CIP (purity ≥99%) procured from EMS pharmaceuticals (Brazil) were applied as adsorbate, and ultrapure water was used for preparing all working standards, except otherwise stated. No adjustment in any way was carried out on the pH of each pharmaceutical solution. **Table 1** summarizes the physicochemical properties of the studied pharmaceuticals.

To prepare individual drug samples, about 100 mg of each of IBP or CIP was separately mixed with ultrapure water containing 1% methanol as a stock solution and then made up to 1000 ml. At 222 nm and 274 nm of absorption wavelength, the

concentrations of both IBP and CIP were quantified respectively by molecular spectroscopy, using a UV-Vis spectrophotometer (Agilent Cary 3500, USA), from which other working standards were prepared.

4. Batch adsorption procedure

Batch adsorption studies were performed to examine the influence of contact time, initial drug concentration, solution pH, adsorbent dosage, and temperature on removal of IBP and CIP by BT. Initially, 0.125 g of BT in 50 mL of 10 mg/L IBP/CIP solution was agitated for 24 hours on a magnetic stirrer at room temperature of 28±2°C and at pH of 7.

Each mixture was subjected to centrifugation for 20 minutes at 600 rpm, filtered after being agitated, and the resulting filtrates were analyzed for IBP and CIP concentrations using UV-Vis spectrophotometer (Agilent Cary 3500, USA) at wavelengths of 222 nm and 274 nm, respectively. From equations (1) and (2), adsorption capacity and removal efficiency of BT for IBP/CIP uptake were estimated.

$$q_e = (C_i - C_e)\frac{V}{m} \qquad (1)$$

$$\%Removal = \frac{C_i - C_e}{C_i} \times 100 \qquad (2)$$

where adsorption capacity of BT is denoted as q_e (mg/g) while C_i and C_e (mg/L) represents initial and equilibrium concentrations of IBP/CIP, respectively. V (mL) denotes the volume of the solution, and m (g) indicates adsorbent's mass.

Kinetic investigation was performed by varying adsorbent-adsorbate interaction time (contact time) from 10 to 240 minutes at aforementioned experimental conditions above. The effect of initial IBP/CIP concentrations ranging from 10 to 100 mg/L was evaluated by agitating 0.125 g of BT in 50 ml of IBP/CIP solution for 24 hours at a temperature of 28±2°C and pH 7. Additionally, the effect of solution pH was tested within the range of 2 to 10, using the same agitation conditions, while the influence of adsorbent dosage was tested by varying it between 0.1 g/L and 0.2 g/L in a 10 mg/L IBP/CIP solution under the same conditions.

Individual adsorption tests were performed in triplicates, with the mean values adopted.

5. Adsorption kinetics and isotherm models

Linear forms of both kinetic (pseudo first order, pseudo second order, and intraparticle diffusion) and isotherm (Langmuir, Freundlich and Temkin) [31] models were applied to describe the kinetic and equilibrium data respectively, for IBP/CIP removal by BT. Details of equations applied to describe both kinetic and equilibrium data are contained in **Table 2**.

To verify suitability and applicability, both kinetic and equilibrium data were subjected to chi-square test ($\chi2$) analysis, using equation (3):

$$\chi^2 = \sum_{n-1}^{n}[\frac{(q_{e\,exp.n} - q_{e\,model.n})^2}{q_{e\,exp.n}} \qquad (3)$$

where, adsorption capacity of BT at equilibrium is represented as $q_{e\,exp}$ (mg/g), $q_{e\,model}$ (mg/g) represents predictions from isotherm and kinetic models which depend on the equilibrium concentration C_e (mg/L), and the total number of observations denoted as n.

6. Thermodynamic Studies

Evaluating thermodynamic parameters is vital for understanding any adsorption process. Gibbs free energy ΔG^0 (kJmol^{-1}), enthalpy change ΔH^0 (Jmol^{-1}) and entropy change ΔS^0 (Jmol^{-1}K^{-1}) were all evaluated within 293 K - 323 K for IBP/ CIP removal by BT in aqueous solutions at similar experimental conditions described for other adsorption experiments above, and according to equations (4) to (6) [33].

$$K = \frac{C_0 - C_e}{C_e} \qquad (4)$$

$$\ln K_d = \frac{\Delta S^0}{R} - \frac{\Delta H^0}{RT} \qquad (5)$$

$$\Delta G^0 = \Delta H^0 - T\Delta S^0 \qquad (6)$$

where initial and equilibrium drug concentrations are represented as C_o and C_e, respectively the universal gas constant (8.314 J/mol K) denoted as R and absolute temperature (K) represented as T.

7. Molecular simulation methods

Molecular modelling was carried out on IBP/CIP with the sole aim of gaining insight into possible interactions between the absorbent and the drug molecules and also to comprehend IBP/CIP molecular chemical reactivity during the adsorption process. Three-dimensional (3D) structures of IBP and CIP were separately obtained and visualized on Gauss View 6.0. Density function theory (DFT) calculations were performed on the individual drug molecules by applying the Gaussian 09W package for the aim of optimizing molecular structure and calculating the quantum chemical molecular descriptors in addition to the orbital energy (highest occupied molecular orbital energy, E_H –HOMO and lowest unoccupied molecular orbital energy, E_L-LUMO). Geometrical optimization was aimed at attaining most stable configurations of IBP/CIP molecules, as well as to also achieve a minimum energy configuration of the drug molecules. The Becke, three -parameter, Lee-Yang-Parr (B3LYP) level of theory with a base set of 6-31G (d) was

employed to execute the calculations. Values obtained for the HOMO and LUMO energies (E_H and E_L) were utilized for calculating other chemical indices such as energy gap (Δ_{H-L}), electronic chemical potential(μ), Global chemical hardness (η) and overall electrophilicity index (ω), by applying equations (7) – (10) [34, 35] respectively.
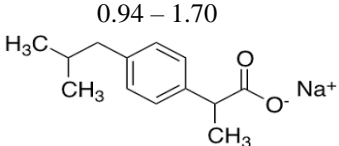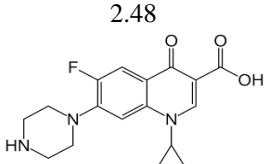
$$\Delta_{H-L} = E_H - E_L \qquad (7)$$

$$\mu = -\frac{E_H - E_L}{2} \qquad (8)$$

$$\eta = \frac{(-E_H - E_L)}{2} \qquad (9)$$

$$\omega = \frac{\mu^2}{2\eta} \qquad (10)$$

Table 1. Physicochemical properties of IBP and CIP used in this study

Parameters	IBP	CIP	Ref
Molecular formula	$C_{13}H_{17}0_2Na$	$C_{17}H_{18}FN_3O_3$	[26, 27]
CAS number	31121-93-4	85721-33-1	[26, 27]
Molecular weight	228.27 g/mol	331.34 g/mol	[26, 27]
Log K_{OW}	3.5-3.97	0.28	[28]
pKa	4.91	Acidic (6.16), basic (8.62)	[29]
Water solubility (25°C)	0.021 mg/ml	$\approx$ 36 mg/ml	[30]
Log P	0.94 – 1.70	2.48	[28]
Structure			[26, 27]

III. RESULTS AND DISCUSSIONS

The morphology of BT is displayed in the SEM micrograph (**Fig. 1a**). Obviously, BT is characterized by a flaky and irregular porous structure- this uncovers some interesting characteristics that could make it a valuable material for removing certain pharmaceuticals, specifically CIP and IBP, from water. This clay has a unique porous structure and a large surface area, both of which are essential for effective adsorption of IBP/CIP.

The XRD pattern of BT is displayed in **Fig. 1b.** Obviously, basal spacing of BT was found to be 10.006 A, with a reflectance intensity of 5.34%. A closer value was reported by Nourmoradi et al. [36], for montmorillonite clay. The XRD analysis of BT sourced from Umuahia North Local Government area of Abia State, Nigeria, highlights its promising characteristics as an adsorbent for IBP and CIP. The analysis shows a significant peak at 28.8898° with a relative intensity of 100%, indicating a well-structured crystalline form, likely montmorillonite, which is known for its high surface area and cation exchange capacity. The d-spacing of 10.006 Å suggests a layered structure that can effectively

accommodate organic molecules. These features enhance the clay's ability to adsorb pharmaceuticals through various mechanisms, such as electrostatic interactions and hydrogen bonding, positioning it as a viable option for removing these drugs from water.

The FTIR analysis of BT in this study provides valuable insights into its functional groups and their interactions with IBP/CIP, which are necessary for evaluating its effectiveness as an adsorbent. Notably, from **Fig. 1c** the peaks observed around 3854 cm^{-1} and 3445 cm^{-1} indicate the presence of hydroxyl (–OH) groups, which are known to enhance the adsorption capacity of BT by promoting hydrogen bonding with the target pharmaceuticals [37]. Furthermore, the peaks in the range of 1645 cm^{-1} and 1402 cm^{-1} may suggest the presence of structural water and various functional groups, such as carbonyl (C=O) and aromatic compounds, which can interact with drug molecules through π-π stacking and electrostatic interactions [38]. Additionally, the notable peak at 811 cm^{-1} is often associated with the bending vibrations of Si-O bonds, further confirming the silicate nature of BT and its potential to effectively adsorb organic contaminants [39].

***Table 2**. Equations of isotherm and kinetic models with definitions*

S/N	Kinetic/Isotherm Model
1	**Pseudo first order**

$$log(q_e - q_t) = log\ q_e - \left(\frac{k_1}{2.303}\right)t$$

Where qe denotes the amount IBP/CIP adsorbed at equilibrium, measured in mg/g, while qt represents the amount adsorbed at any given time, t (sec), also in mg/g. The variable k signifies the rate constant for the pseudo-first-order model.

2	**Pseudo second order**

$$\frac{1}{q_t} = \frac{1}{k_2 q_e^2} + \frac{t}{q_e}$$

Where k_2 signifies the rate constant for the pseudo second order model, and other quantities same as the pseudo first order kinetic model

3	**Intraparticle diffusion**

$$q_t = k_{id} t^{\frac{1}{2}} + C$$

Where the rate of intraparticle diffusion kinetic model is denoted as k_{id} (g/mg-h)

4	**Langmuir**

$$\frac{C_e}{q_e} = \frac{C_e}{Q_m} + \frac{1}{bQ_m}$$

Where Ce (mg/L) represents IBP/CIP concentration, qe (mg/g) indicates equilibrium adsorption capacity of BT, b (L/mg) is the Langmuir constant and Qm (mg/g) denotes the maximum capacity of the adsorbent.

5	**Freundlich**

$$ln\ q_e = ln\ k_f + \frac{1}{n}\ lnC_e$$

Where q_e represents the adsorption capacity of BT measured in mg/g, and Ce denotes the concentration of the adsorbate at equilibrium, expressed in mg/L.

6	**Temkin**

$$q_e = \frac{RT}{b}lnA + \frac{RT}{b}lnC_e$$

Where A (L·mg⁻¹) and b represent the constants of the Temkin isotherm, with R equal to 0.0083 kJ·mol⁻¹·K⁻¹ and T indicating the temperature in Kelvin (K).
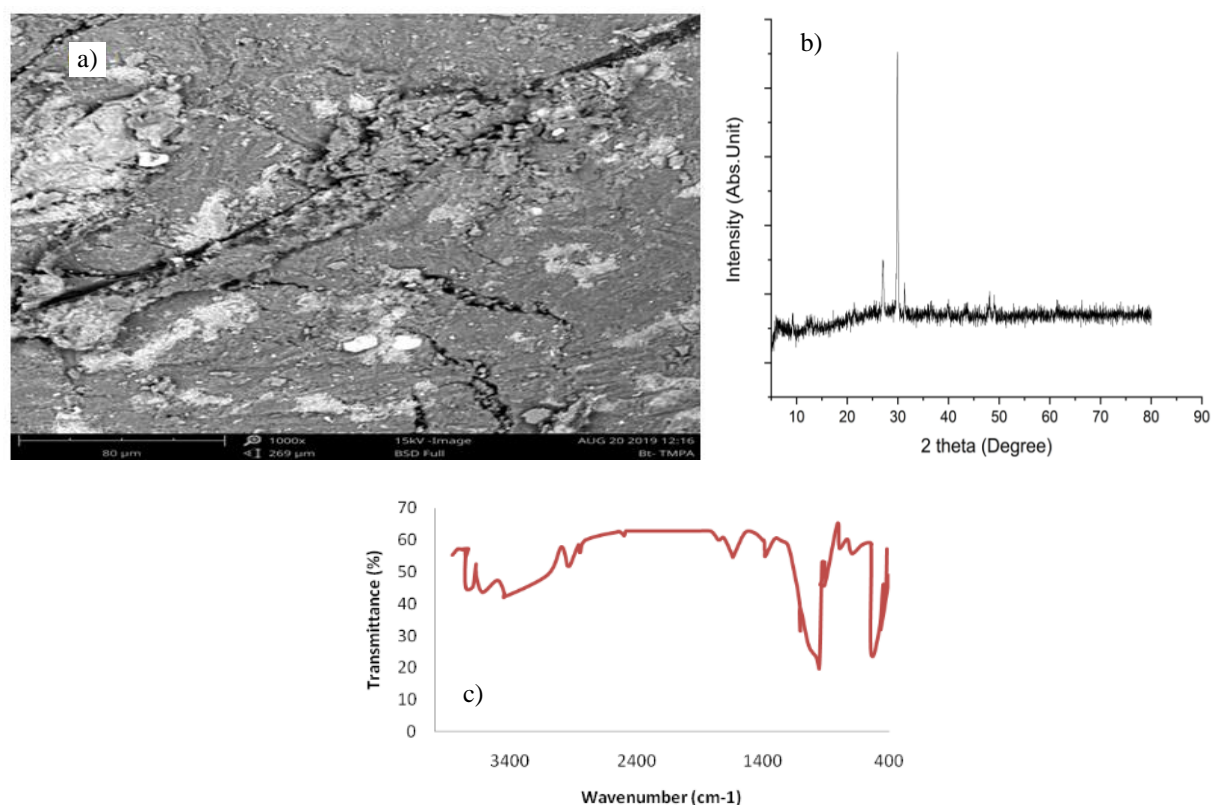
***Figure 1.** SEM micrograph (a), XRD diffractogram (b) and FTIR spectra (c) of BT*

1. Effect of various parameters on adsorption

A. Contact time

The adsorption of IBP/CIP on BT was examined within 10 to 240 minute intervals of adsorbent-adsorbate interaction time. **Fig. 2(a)** presents the effect of contact time on adsorption capacity and percentage removal efficiency of BT for IBP/CIP. Adsorption of the pharmaceuticals were extremely swift within 90 minutes of interaction time, resulting in 78.6% and 47.7%; and 3.14 mg/g and 1.91 mg/g, removal efficiency and adsorption capacities for IBP and CIP, respectively. Observed rapid adsorption of pharmaceuticals by BT may be due to more available vacant binding sites present on BT surface. Adsorption of the pharmaceuticals continued slowly thereafter, until equilibrium was attained at 240 minutes maximum contact time, corresponding to 87.7% and 59.5% removal efficiency and 3.51 mg/g and 2.38 mg/g adsorption capacities for IBP and CIP respectively. Similar adsorption trends have been previously reported for adsorption of CIP and IBP employing natural clay as well as other adsorbents [1, 15, 40, 41].

B. Initial drug concentration

Fig. 2(b) represent the influence of initial IBP/CIP concentration (10 - 100 mg/L) on IBP/CIP adsorption onto BT. Obviously, as initial drug concentration increase, the adsorption capacity also increased as well for both IBP and CIP. When the initial IBP/CIP concentration was observed as 100 mg/L, about 89.9% and 80.9% removal efficiency, corresponding to 35.98 mg/g and 32.37 mg/g adsorption capacities for IBP and CIP respectively were recorded. Although the percentage removal efficiency varied at different initial drug concentrations, 93.1% and 88.1% maximum removal efficiency was recorded at the initial IBP/CIP concentration of 60 mg/L. There may be attributed to more available vacant sites on adsorbent's surface for effective binding of drug molecules at decreased initial drug concentrations, and as the concentration rises, the number of available active sites reduces, resulting to a high adsorption capacity and, ultimately, the observed discrepancy in the percentage removal efficiency [42]. At initial CIP concentration of 50 mg/L, about 99.3% removal of CIP by Aleppo bentonite was reported by Hicham et al. [42].

C. Solution pH

The effect of variation of pH from 2-10 on IBP/CIP removal by BT is presented in **Fig. 2(c)**. Various studies [8, 43] have documented the impact of pH on pharmaceuticals adsorption. Mostly, pharmaceutical adsorption is affected by solution pH. As seen in **Fig. 2(c)**, ibuprofen was best removed within pH range of 2 and 4, resulting in high adsorption capacity and removal efficiency. The pKa of IBP is 4.91, and as the pH value becomes basic, the dissociation degree of the surface groups of both IBP and BT turns negative [43]. IBP removal by BT could result in electrostatic repulsion which in turn brings about decreased adsorption capacity as pH exceeds 4. Therefore, IBP was better sorbed at pH of 4, resulting in a removal percentage of 86.6% (**Fig. 2c**). A comparable outcome was documented by Khazri and co-workers [43], who applied natural clay for ibuprofen, naproxen, and carbamazepine removal in aqueous solutions. On the other hand, CIP was better adsorbed by the BT between the pH range of 4 to 6. At pH of 6, CIP displays a positive charge, promoting electrostatic attraction between the adsorbent and the drug molecule, thereby resulting in increased adsorption. However, it is also worth noting that electrostatic repulsion between adsorbent and drug molecules becomes eminent at pH less than pKa of 6.16 and pKa value found to be higher than 8.62, which leads to decreased adsorption capacity [44]. In addition, CIP displayed higher solubility at acidic pH, and this in turn accounts for lower adsorption at decreased pH. At pH of 6, increased adsorption capacity of 2.72 mg/g and removal efficiency of 67.9% indicates that the porosity of BT was in charge of the highest adsorption of CIP, and slso, potential electrostatic interaction via Van der Waals forces that took place on the active sites of the BT surface. Similar to the case of IBP, protonation of the amino group results in positively charged species and deprotonation of the carboxylic group results to a negative charge species at pH of 6 for CIP. Electrostatic repulsion reduces adsorption efficiency at pH less than 6 and higher than 6 [8, 44]. This information is important for IBP and CIP removal from wastewater, since pH of 6 to 8 have been mostly reported for wastewater [44].

D. Adsorbent dosage

Different pollutants require different kinds of adsorbents, and most times, the type and quantity of adsorbent required for adsorption of a particular adsorbate depends on the adsorbents' physicochemical properties. BT's specific surface area and CEC value were calculated in this study to be 327 m^2/g and 30.94 meq/100 g, respectively.

The influence of adsorbent dosage (0.1 g/L to 0.2 g/L) on IBP/CIP removal by BT under optimum experimental conditions is illustrated in **Fig. 2 (d-e).** Obviously, removal of IBP and CIP by BT followed a similar trend. Adsorption capacity increased proportionally with adsorbent dosage. This increment in adsorption capacity suggests availability of sufficient active binding sites on BT surface consequent upon adsorbent increment, which in-turn resulted in an increment in percentage removal of IBP and CIP by BT. Up to 90.2% and 66.9% removal was recorded for IBP and CIP respectively at maximum adsorbent dosage of 0.2 g/L. Jara-Cobos et al. [8], reported 62.7% and 90.5% removal of ciprofloxacin by pillar calcium bentonite (BCP) and pillared sodium bentonite (BSP) respectively. Ghemit et al. [15] also reported similar trend (although with greater adsorption capacity) for diclofenac and ibuprofen removal by organobentonite.
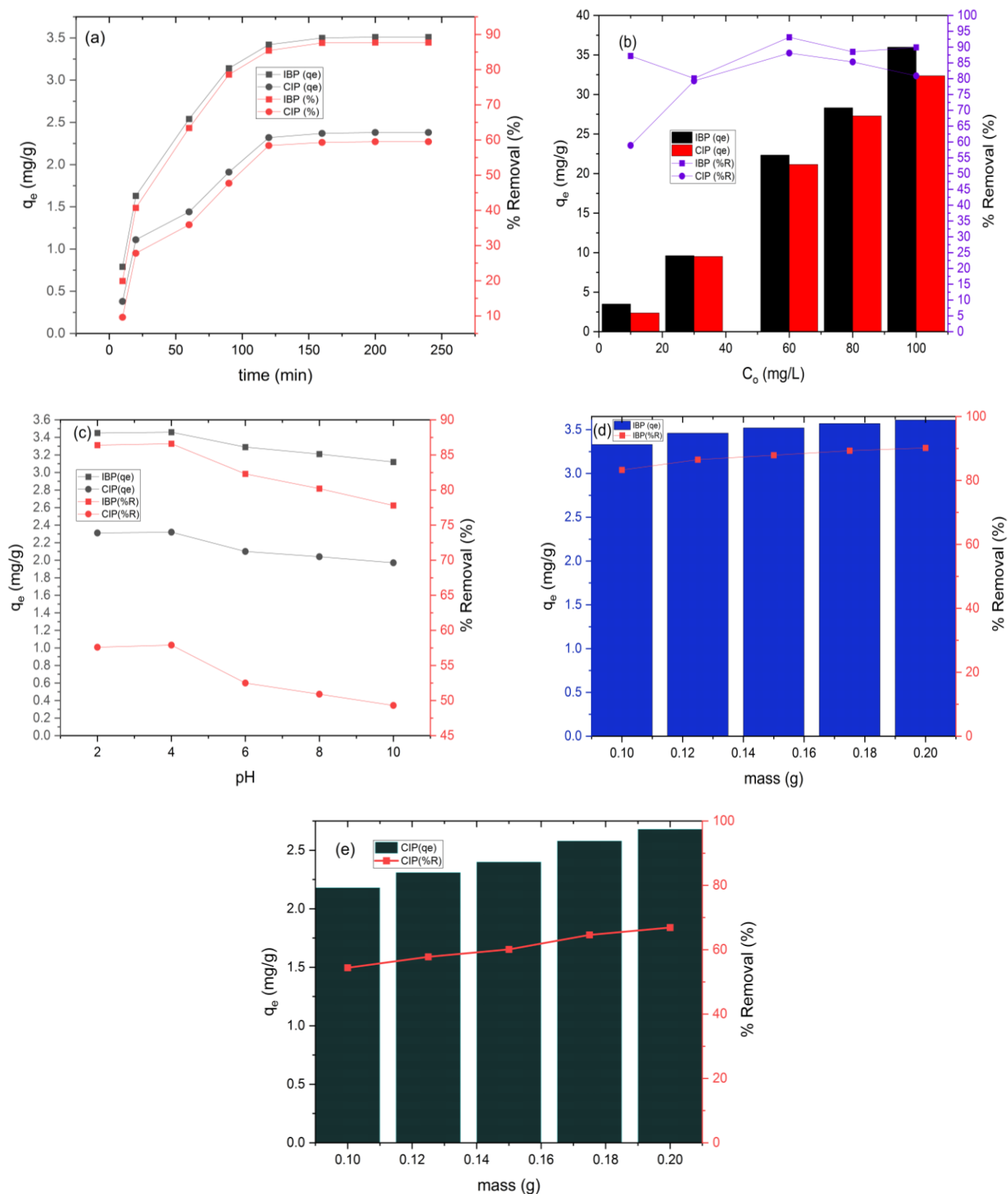
Figure 2. *Effect of (a) contact time (m = 0.125 g, V = 50 ml, C_0 = 10 mg/L, t = 24h, T = 28±2°C, pH =7); (b) initial IBP/CIP concentration (m = 0.125 g, V = 50 ml, t = 24h, T = 28±2°C, pH =7); (c) pH (m = 0.125 g, V = 50 ml, C_0 = 10 mg/L, t = 24h, T = 28±2°C); (d) adsorbent dosage- IBP (V = 50 ml, C_0 = 10 mg/L, t = 24h, T = 28±2°C, pH =7) and (e) adsorbent dosage CIP (V = 50 ml, C_0 = 10 mg/L, t = 24h, T = 28±2°C, pH =7) on IBP/CIP removal by BT (CEC=30.94 meq/100 g).*
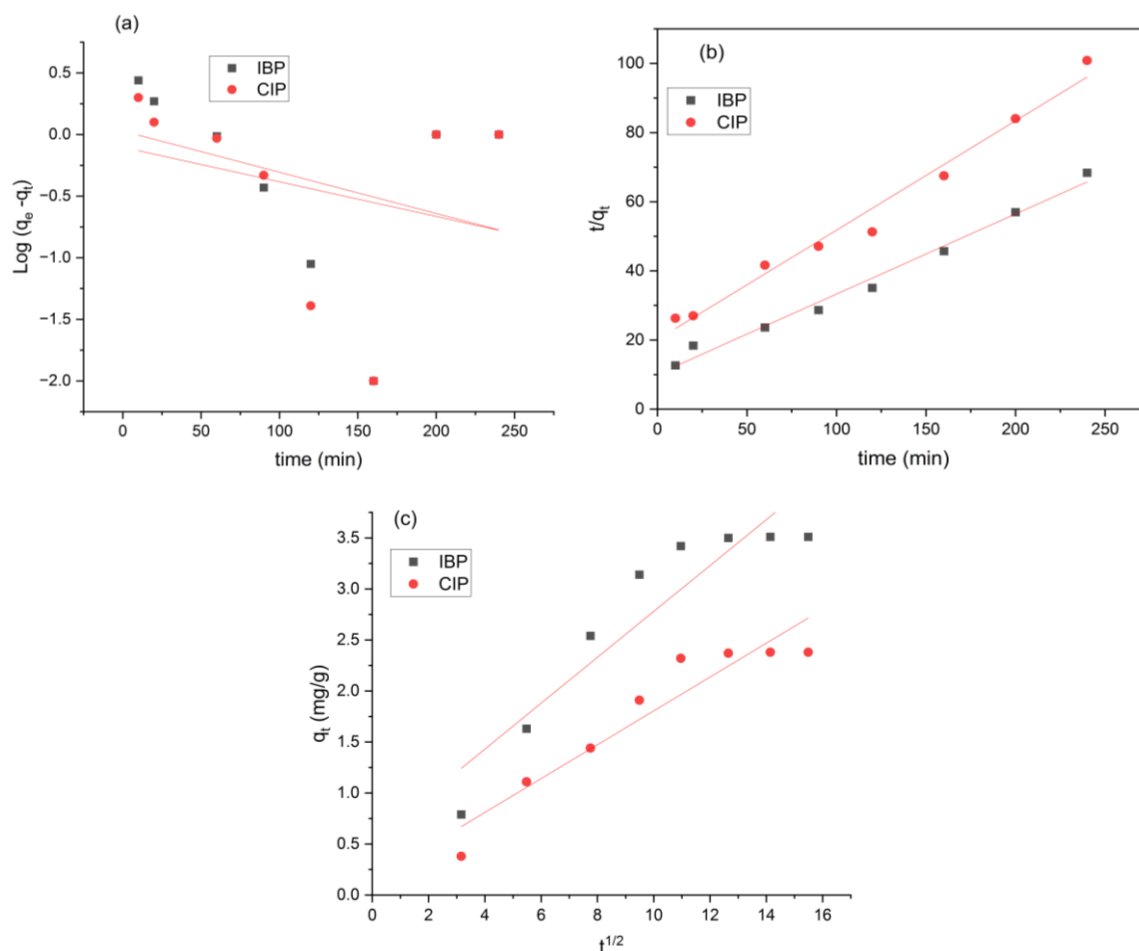
Figure 3. *Linear plots of (a) Pseudo first order model, (b) Pseudo second order model and (c) Intraparticle diffusion model for IBP/CIP removal onto BT*

2. Adsorption kinetics

The kinetic data were tested by pseudo first order, pseudo second order, and intraparticle diffusion kinetic models, with individual kinetic plots and parameters presented in **Fig. 3(a-c)** and **Table 3** respectively. Comparatively, higher R^2 values were recorded for the pseudo second order kinetic model, in the removal of both pharmaceuticals by BT, implying that chemical adsorption may be the rate-limiting step for the sorption process [15]. Similarly, diclofenac and Ibuprofen has been efficiently sorbed by organobentonite from aqueous solution [15]. The kinetic data involving ciprofloxacin removal by natural and hydrolyzed bentonite in aqueous medium was shown to be better fitted to a pseudo second order kinetic model in another investigation [1]. Additionally, 2.15 mg/g and 3.33 mg/g; and 3.51 mg/g and 2.38 mg/g; calculated (q_{ecal}) and experimental (q_{eexp}) q_e values obtained for CIP and IBP respectively for the pseudo second order model were quite close (**Table 3**), compared to values obtained for other kinetic models, suggesting that the

pseudo second order kinetic model gave a better fit to the kinetic data.

3. Adsorption isotherm

Frequently applied isotherm models (Langmuir, Freundlich, and Temkin) were used to test the equilibrium data. The equations for these isotherm models, as well as other information, are presented in the previous section. Linear plots of these isotherms are presented in **Fig. 4(a-c)**, and different isotherm parameters evaluated presented in **Table 4**. At concentration range of 10 - 100 mg/L and at 28±2°C, adsorption isotherm experiment was conducted. The Freundlich isotherm model fitted better to the equilibrium data, following highest recorded values for correlation coefficient, R^2 for both pharmaceuticals, compared to the Langmuir and Temkin isotherms. This implies multi-layer adsorption of IBP/CIP onto the BT surface. Comparatively, Langmuir and Temkin models also produced high R^2 values of 0.985 (IBP) and 0.902 (CIP) respectively, but Chi-square test analysis χ^2 displayed much lower values for Freundlich isotherm compare to other tested isotherm models

for both pharmaceuticals. A strong interaction bond between absorbent and absorbate molecules is indicated by n larger than 1, as per the Freundlich isotherm. Therefore, n values obtained as 1.37 and 1.42 for both IBP and CIP respectively, imply maximum adsorption of these drug molecules onto BT surface.

Table 3. Kinetic parameters for IBP and CIP adsorption onto BT

Kinetic Models	Parameters	Adsorbate	
		IBP	*CIP*
Pseudo first Order	Constant of pseudo first order (k_1)	0.013	0.009
	Calculated adsorption capacity for the pseudo first order (q_e)	1.07	1.27
	Correlation coefficient of pseudo first order (R^2)	0.118	0.080
Pseudo second Order	Constant of pseudo first order (k_2)	0.009	0.011
	Calculated adsorption capacity for the pseudo second order ($q_{e\ cal}$)	3.33	2.15
	Experimental adsorption capacity ($q_{e\ exp}$)	3.51	2.38
	Correlation coefficient of pseudo second order (R^2)	0.986	0.980
Intra-particle diffusion	Rate of intraparticle diffusion kinetic model (K_{id})	0.22	0.17
	Constant for intraparticle diffusion kinetic model (C)	0.53	0.15
	Correlation coefficient for intraparticle diffusion kinetic model (R^2)	0.864	0.899

Table 4. Isotherm Parameters Evaluated for IBP/CIP Adsorption onto BT

Isotherm models	Parameters	IBP	CIP
Langmuir	Langmuir adsorption capacity, Q_m (mg/g)	14.71	33.33
	Langmuir constant, b (L/mg)	0.069	0.039
	Corelation coefficient (R^2)	0.985	0.779
	Chi-square (χ^2)	12.31	6.124
Freundlich	Freundlich constant K_f	15.64	4.18
	Freundlich constant (n)	1.37	1.43
	Correlation coefficient (R^2)	0.979	0.975
	Chi-square (χ^2)	0.441	1.061
Temkin	Temkin's constant (A)	1.08	3.30
	Temkin's constant (B) (L/mg)	0.186	0.123
	Correlation coefficient R^2	0.672	0.902
	Chi-square (χ^2)	4.162	1.994
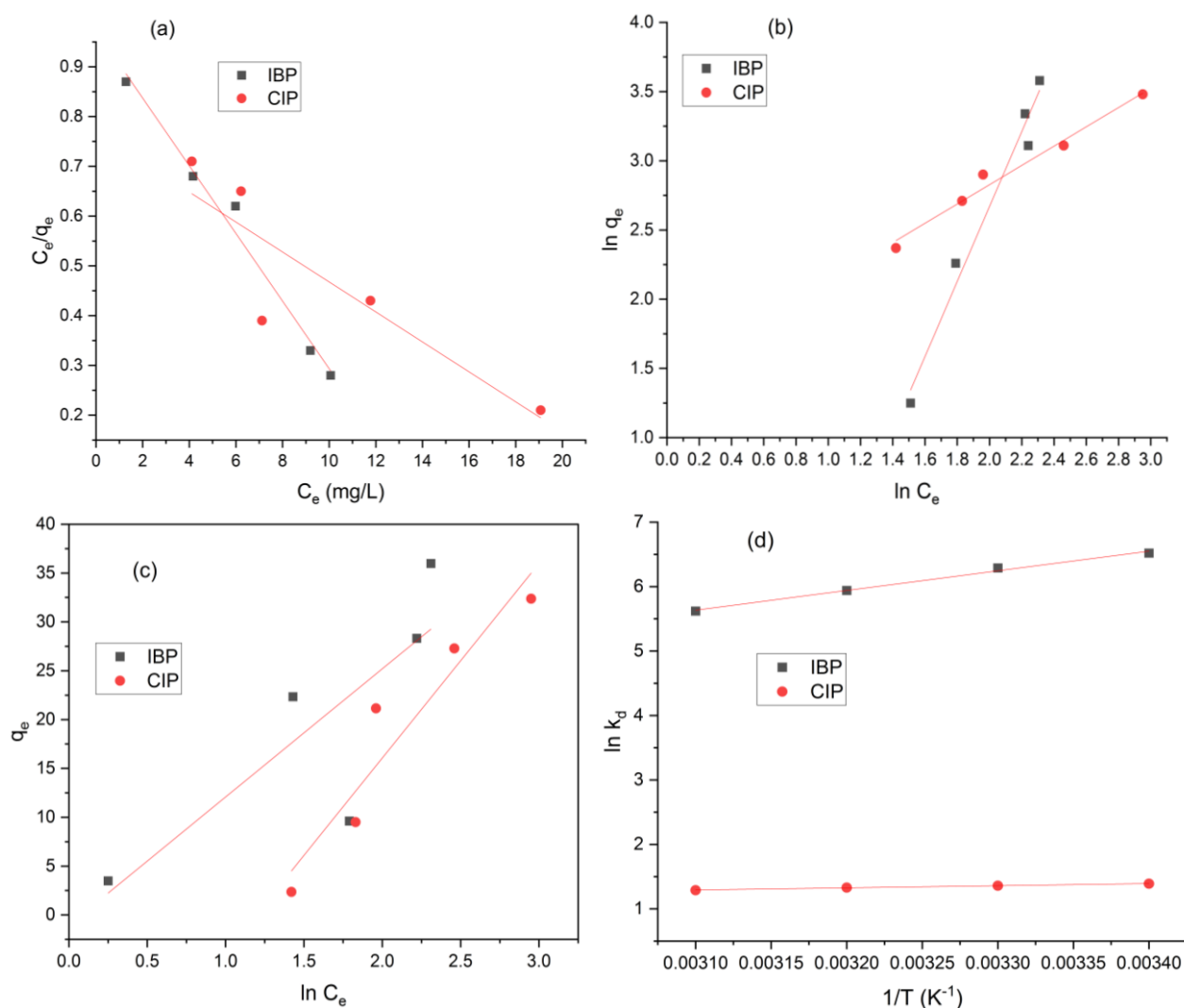
Figure 4. *Linear plots of adsorption isotherm models (a) Langmuir, (b) Freundlich and (c) Temkin :(m = 0.125 g, V = 50 ml, t = 24h, T = 28°C, pH =2); and (d) Plots of ln k_d against 1/T for IBP/CIP removal by BT*

4. Thermodynamic assessment

Table 5 lists the thermodynamic parameter values that were determined for this investigation, and **Fig. 2(d)** shows the graph of ln K_d against 1/T for IBP/CIP uptake by BT in an aqueous medium. It is noticeable that adsorption capacities for IBP and CIP decreased continuously as temperature increased (**Table 5.**). In other words, adsorption of IBP and CIP is favourable at low temperatures. At 293 K, 3.47 mg/g and 2.32 mg/g were recorded as maximum adsorption capacities for IBP and CIP respectively.

Thermodynamically, negative values were obtained for Gibbs free energy (ΔG^0) for both pharmaceuticals and these values increased negatively as temperature increased- an indication of a spontaneous process [44]. Positive values of enthalpy change (ΔH^0) which were < 40 KJ/mol suggest that IBP/CIP adsorption onto BT was an endothermic process involving physisorption [33, 42]. Previously, data from kinetic studies revealed that BT's absorption of IBP and CIP followed a pseudo second order kinetic model, suggesting primary rate-controlling step to be chemical adsorption. However, this is in contrast to data from thermodynamic analysis. Typically, adsorption process involves numerous steps, and while kinetic studies can furnish vital information regarding reaction mechanisms, categorizing this intricate process as chemisorption is insufficient. However, adsorption isotherm and thermodynamic investigation is required to gain more insight into the adsorption mechanism. Studies have also shown that both physical and chemical processes may occur together in adsorption systems [43]. It is important

to note that numerous researchers have previously reported similar results but with no explanation, until it was proposed and reported by Baraka [45], that physisorption and chemisorption are both valid for the pseudo second order kinetic model. For IBP and CIP, the entropy change (ΔS^0) was 1.72 and 0.77,

respectively. These observed positive values suggest the existence of increased randomness during the adsorption of IBP and CIP onto BT, confirming that the adsorption of both pharmaceuticals onto BT was favourable [42].

Table 5. Thermodynamic parameters for IBP/CIP removal by BT

BT/ Adsorbate	ΔS^0 (J/mol·k)	ΔH^0 (J/mol)	ΔG^0 (kJ/mol)				qe (mg/g)			
			293K	303K	313K	323K	293K	303K	313K	323K
BT/IBP	1.72	8.56	-1.12	-2.22	-2.99	-3.02	3.47	3.45	3.42	3.39
BT/CIP	0.77	18.34	-2.78	-2.98	-3.76	-3.99	2.32	2.31	2.28	2.26

5. DFT study

In this study, the molecular and electronic properties of IBP and CIP were the focus of the DFT calculations performed, to obtain greater insight into their distinct adsorption behaviour on BT. Geometrical optimization of IBP/CIP was carried out using B3LYP with a base set of 6-31G(d), from which different conformations of the drug molecules were obtained (**Figure A1 and A2** of Appendix), and more stable conformers with lower molecular energies for both IBP and CIP (**Fig. 5 (a-b)**) were adopted. Antonelli et al. [21] and Wazzan, [46] verified similar results for ciprofloxacin (CIP) and ibuprofen (IBP) respectively. Obviously, the optimized structure of CIP is characterized by twisting of the aromatic rings due to repulsive interactions between the aromatic rings. Again, the optimized IBP molecule indicates a planer geometry due to a situated single aromatic ring, which gives room for a large part of the molecules' skeleton to lie on the same plane thereby accounting for a very lower electrostatic repulsion within the molecule. It is important to mention that the obtained optimized structure of IBP/CIP corresponding to configurations of minimum energy was confirmed by vibrational analysis and stability calculation and details of values obtained for bond lengths and angles for individual pharmaceuticals are contained in **Table A1 and A2** (Appendix).

Significantly, an organic pollutant's size and shape can impair accessibility to the absorbent surface's active site, leading to subpar adsorptive performance [35, 47]. When large sized molecules block adsorption sites on adsorbent surfaces, hindering effective binding, steric hindrance occurs [35, 47-50]. CIP is significantly longer (13.319 Å) and has a larger molecular weight (228.6 g/mol) than IBP (12.527 Å), as shown in **Table 1** and **Fig. 5(a-b)**. Comparatively, CIP may display a greater steric hindrance than IBP, making some of the active site on BT surface unable to sorb CIP molecules effectively. This accounts for the greater adsorption

capacity of BT recorded for IBP, with less adsorption efficiency observed for CIP. **Table 6** shows the DFT-based reactivity descriptors that were acquired for IBP and CIP.

The frontier molecular orbital energies are crucial for understanding the molecular reactivity of distinct drug species and can be obtained more easily through geometrical optimization [46]. The primary components of these frontier molecular orbital energies are the lowest unoccupied molecular orbital energy (E_L – LUMO) and the highest occupied molecular orbital energy (E_H – HOMO). **Fig. 5(c-d)** shows the three-dimensional (3D) contour plots of the HOMO and LUMO for IBP and CIP. The propensity of a molecule to give electrons is measured by the HOMO energy levels (E_H). A molecule can give electrons more readily as its value destabilizes, or becomes less negative. Conversely, a molecule's propensity to receive electrons is measured by the LUMO energy levels (E_L) [45, 51]. According to **Table 6**, IBP presented a higher value for E_H and E_L compared to CIP, which was 0.96 eV and 0.33eV lower. Thus, the IBP is more capable of releasing electrons, but it is more resistant to gaining electrons [46]. The HOMO-LUMO energy gap (Δ_{H-L}) serves as a measure of the kinetic stability and reactivity of molecules, defined as the difference between the HOMO and LUMO orbital energies. Generally, a low value of Δ_{H-L} implies that such a molecule is reactive and vice versa [52]. Therefore, both pharmaceuticals presented lower values of Δ_{H-L}. Although CIP was less than IBP by 1.69 eV, suggesting that it could be a more reactive pharmaceutical than IBP. The values of Δ_{H-L} found as 5.88 eV and 4.19 eV for IBP and CIP correspond to those reported in other studies [21, 46]. Generally, electrochemical potential (μ) is the degree to which an electron has a tendency to escape from a molecule [21]. IBP has a lower tendency to retain electrons than CIP, as evidenced by their respective electrochemical potentials of 3.45 eV and 3.34 eV. Global chemical hardness (η), which measures resistance to changing electronic density, is used to

quantify molecule stability and reactivity [21, 46, 51]. When a molecule is "soft", its electronic density can be easily altered and vice versa. In this study, η values of 2.94 eV for IBP and 2.09 eV for CIP were calculated (**Table 6.**). IBP is expected to showcase a higher difficulty in altering electronic density compared to CIP, judging by the differences in their η values. However, CIP is a softer molecule compared to IBP. The overall electrophilicity index (ω) defines the electron retention capacity. A low value of ω for a molecule signifies that it has a low capacity to retain electrons [51, 53]. IBP displayed a lower value of ω compared to CIP, indicating that the former possesses a lower electron retention capacity.

Analysis involving DFT-based quantum chemical descriptors indicates that IBP exhibits a marginally greater electrophilic character and demonstrates a more significant alteration in electronic density compared to CIP. This is consistent with experimental data from the batch adsorption of IBP/CIP onto BT, which reveal that IBP is more readily eliminated from the solution than CIP. Consequently, this behaviour may account for the observed higher adsorption capacity of IBP relative to CIP under the different experimental conditions examined.
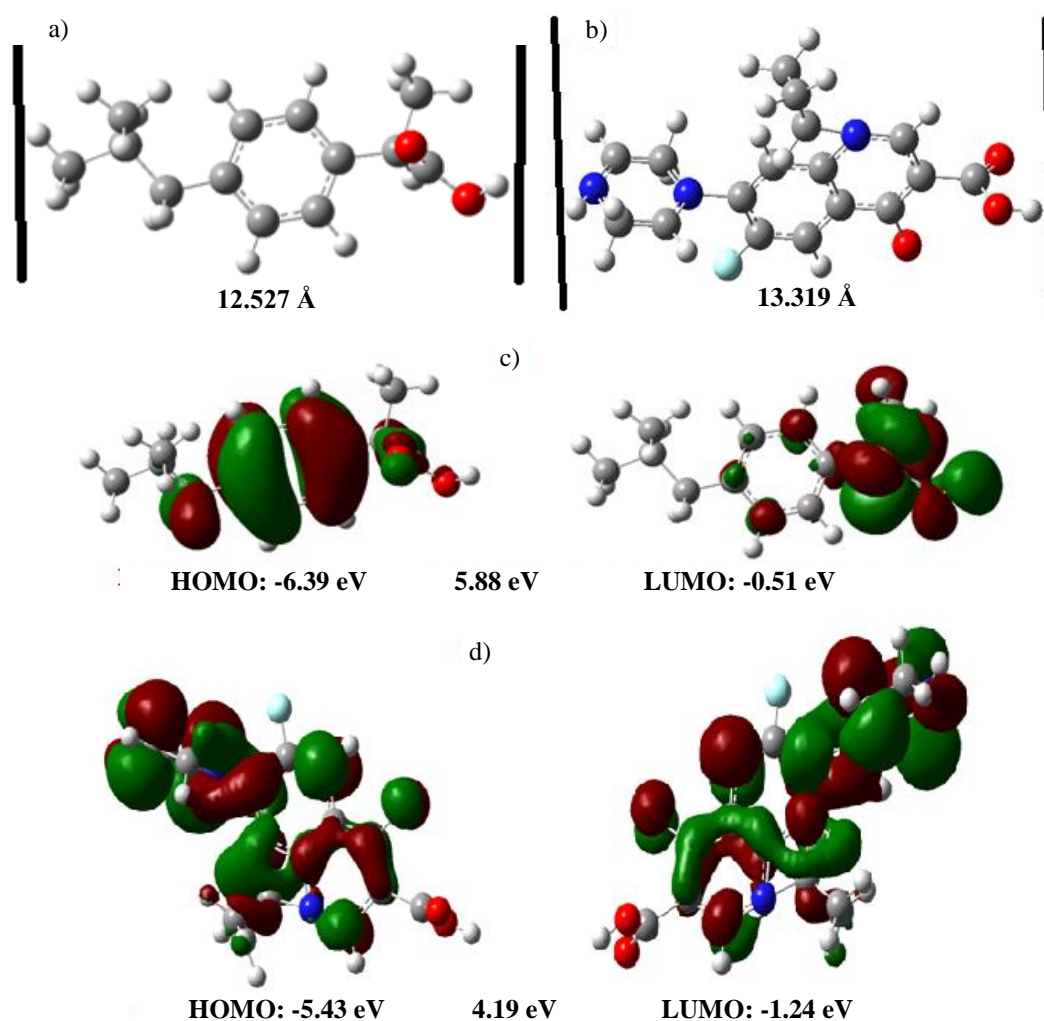
Figure 5. Optimized molecular structures of IBP (a) and CIP (b) calculated at B3LYP/6-31G(d) level of theory; 3-D plots of HOMO and LUMO of IBP (c) and CIP (d) (Red colour: positive phase; Green colour: negative phase)

***Table 6.** Calculated quantum chemical parameters of IBP and CIP by B3LYP/631G(d) approach.*

Quantum chemical parameter	IBP	CIP
HOMO energy (E_H, eV)	-6.39	-5.43
LUMO energy (E_L, eV)	-0.51	-1.24
Energy gap (Δ_{H-L}, eV)	5.88	4.19
Chemical potential (μ, eV)	3.45	3.34
Chemical hardness (η, eV)	2.94	2.09
Electrophilicity index (ω, eV)	2.02	2.67

IV. CONCLUSIONS

In current study, bentonite clay has been successfully applied as suitable adsorbent for comparative adsorption of IBP/CIP from aqueous media. Obviously, the porous structure of the clay accounted for the observed high removal efficiency of both pharmaceuticals, even though the clay was not modified with any form of surfactant. Experimental conditions like variations in adsorbent dosage, contact time, temperature, pH, and initial IBP/CIP concentration greatly influenced adsorption capacity and removal efficiency of both pharmaceuticals by BT. Thermodynamic analyses suggest that the adsorption of both pharmaceuticals onto BT is feasible, spontaneous, endothermic, and characterized by randomness, indicating a physisorption mechanism. The Freundlich isotherm and the pseudo-second-order kinetic model are the most effective for representing the isotherm and kinetic data, respectively. In contrast to CIP, density functional theory (DFT) studies indicate that IBP demonstrates greater electrophilicity, enhancing its ability to modify its electronic density. This observation is supported by experimental findings that shows that IBP is adsorbed more effectively from aqueous solutions onto BT.

In sum, BT have been known to be less toxic (eco-friendly), cheap and readily available and this makes it a potential adsorbent for removal of emerging contaminants in large scale scenarios as seen in this study.

ACKNOWLEDGEMENT

AUTHOR CONTRIBUTIONS

K. E. Onwuka: Conceptualized and discussed and finalized the article

A. A. Ahuchaogu: Conceptualized and discussed and finalized the article

O. C. Atasie: Analysis and interpretation of data

N.B Nwosu: Analysis and interpretation of data

V. C. Oguike: Instrumental analysis

A. C. Nwosu: Instrumental analysis

J. O. Nwagba: Revised article

DISCLOSURE STATEMENT

ORCID

K.E. Onwuka http://orcid.org/0000-0001-8408-0949

A.A. Ahuchaogu http://orcid.org/0000-0002-6412-7487

O.C. Atasie http://orcid.org/0009-0004-4653-9762

V.C. Oguike http://orcid.org/0000-0002-9009-2951

N.B. Nwosu http://orcid.org/0000-0002-1562-7258

NOMENCLATURE

Symbol/Abbreviation	Definition	Units
A	Temkin isotherm constant related to adsorption energy	$L\cdot mg^{-1}$
AOPs	Advanced Oxidation Processes	-
BT	Bentonite clay	-
b	Langmuir constant related to adsorption energy	$L\cdot mg^{-1}$
C	Intraparticle diffusion constant	$mg\cdot g^{-1}$
C_e	Equilibrium concentration of adsorbate in solution	$mg\cdot L^{-1}$
C_0	Initial concentration of adsorbate in solution	$mg\cdot L^{-1}$
CEC	Cation Exchange Capacity	$meq\cdot 100g^{-1}$
CIP	Ciprofloxacin	-
DFT	Density Functional Theory	-
ΔG	Gibbs free energy change	$kJ\cdot mol^{-1}$
ΔH	Enthalpy change	$J\cdot mol^{-1}$
ΔS	Entropy change	$J\cdot mol^{-1}\cdot K^{-1}$
E_H- HOMO	Highest Occupied Molecular Orbital energy	eV
E_L-LUMO	Lowest Unoccupied Molecular Orbital energy	eV
Δ_{H-L}	| HOMO-LUMO energy gap	eV
EC	Emerging Contaminants	-
FTIR	Fourier Transform Infrared Spectroscopy	-
IBP	Ibuprofen	-
K	Thermodynamic equilibrium constant	-
K_d	Distribution coefficient	-
K_F	Freundlich constant related to adsorption capacity	$mg\cdot g^{-1}$
K_1	Pseudo-first-order rate constant	min^{-1}
K_2	Pseudo-second-order rate constant	$g\cdot mg^{-1}\cdot min^{-1}$
k_{id}	Intraparticle diffusion rate constant	$mg\cdot g^{-1}\cdot min^{-1/2}$
Log K_{OW}	Octanol-water partition coefficient	-
m	Mass of adsorbent	g
n	Freundlich constant related to adsorption intensity	-
PPCPs	Pharmaceuticals and Personal Care Products	-
Q_m	Maximum monolayer adsorption capacity (Langmuir)	$mg\cdot g^{-1}$
q_e	Equilibrium adsorption capacity	$mg\cdot g^{-1}$
q_t	Adsorption capacity at time t	$mg\cdot g^{-1}$
R	Universal gas constant	8.314 $J\cdot mol^{-1}\cdot K^{-1}$
R^2	Coefficient of determination	-
SEM	Scanning Electron Microscopy	-
T	Absolute temperature	K
t	Contact time	min
V	Volume of solution	mL
XRD	X-ray Diffraction	-
X^2	Chi-square statistic	-
μ	Electronic chemical potential	eV
η	Global chemical hardness	eV
ω	Electrophilicity index	eV

REFERENCES

[1] L. Jara-Cobos, D. Abad-Delgado, J. Ponce-Montalvo, M. Menendez, M. E. Peñafiel, Removal of ciprofloxacin from an aqueous medium by adsorption on natural and hydrolyzed bentonites, Frontiers in Environmental Science 11 (2023) p. 1239754. https://doi.org/10.3389/fenvs.2023.1239754

[2] R. Gondi, S. Kavitha, R. Y. Kannah, O. P. Karthikeyan, G. Kumar, V. Kumar Tyagi et al., Algal-based system for removal of emerging pollutants from wastewater: A review, Bioresource Technology 344 (2022) p. 126245. https://doi.org/10.1016/j.biortech.2021.126245

[3] A. Peña-Álvarez, A. Castillo-Alanís, Identificación y cuantificación de contaminant esemergent esenaguas residual espor microextracción enfasesólida-cromatografía de gases- espectrometría de masas (MEFS-CG-EM), TIP RevistaE specializadaen Ciencias Químico-Biológicas 18 (1) (2015) pp. 29–42.
https://doi.org/10.1016/j.recqb.2015.05.003

[4] G. González, B. R. Berenice, E. A. Flores-Contreras, R. Parra-Saldívar, M. Hafiz, N. Iqbal, Bio-removal of emerging pollutants by advanced bioremediation techniques, Environmental Research 214 (2022) p. 113936.
https://doi.org/10.1016/j.envres.2022.113936

[5] C. Cuerda, E. Manuel, F. M. Alexandre-Franco, C. Fernández-González, Advanced oxidation processes for the removal of antibiotics from water. An overview, Water 12 (1) (2019) p. 102.
https://doi.org/10.3390/w12010102

[6] J. Martín, M. Orta, S. Medina-Carrasco, J. L. Santos, I. Aparicio, E. Alonso, Evaluation of a modified mica and montmorillonite for the adsorption of ibuprofen from aqueous media, Applied Clay Science 171 (2019) pp. 29–37.
https://doi.org/10.1016/j.clay.2019.02.002

[7] Y. Yang, Y. S. Ok, K. H. Kim, E. E. Kwon, Y. F. Tsang, Occurrences and removal of pharmaceuticals and personal care products (PPCPs) in drinking water and water/sewage treatment plants: a review, Science of The Total Environment 596 (2017) pp. 303–320.
https://doi.org/10.1016/j.scitotenv.2017.04.102

[8] L. Jara-Cobos, M. E. Peñafiel, C. Montero, M. Menendez, V. Pinos-Vélez, Ciprofloxacin removal using pillared clays, Water 15 (2023) p. 2056.
https://doi.org/10.3390/w15112056

[9] S. Elhadad, Z. Orban, F. Attila, Pandemic COVID-19: challenge strategic decisions on building in Egypt, Acta Technica Jaurinensis, Vol. 16, No. 2, pp. 83-89, 2023.
https://doi.org/10.14513/actatechjaur.00696

[10] D. Zheng, M. Wu, E. Zheng, Y. Wang, C. Feng, J. Zou, M. Juan, X. Bai, T. Wang, Y. Shi, Adsorption and oxidation of ciprofloxacin by a novel layered double hydroxides modified sludge biochar, Journal of Colloid and Interface Science 625 (2022) pp. 596–605.
https://doi.org/10.1016/j.jcis.2022.06.046

[11] H. R. Busar, T. Poiger, M. D. Müller, Occurrence and fate of the pharmaceutical drug diclofenac in surface waters: rapid photodegradation in a lake, Environmental Science & Technology 32 (22) (1998) pp. 3449–3556.
https://doi.org/10.1021/es980036q

[12] G. R. Boyd, H. Reemtsma, D. A. Grim, S. Mitra, Pharmaceuticals and personal care products (PPCPs) in surface and treated waters of Louisiana, USA and Ontario, Canada, Science of The Total Environment 311 (1-3) (2003) pp. 135–149.
https://doi.org/10.1016/S00489697(03)00141-4

[13] S. Joss, A. Zabczynski, B. Göbel, D. Hoffmann, C. S. Löffler, T. A. McArdell, A. Ternes, H. Thomsen, H. Siegrist, Biological degradation of pharmaceuticals in municipal wastewater treatment: proposing a classification scheme, Water Research 40 (8) (2006) pp. 1686–1696.
https://doi.org/10.1016/j.watres.2006.02.014

[14] S. Esplugas, D. M. Bila, L. Gustavo, T. Krause, M. Dezotti, Ozonation and advanced oxidation technologies to remove endocrine disrupting chemicals (EDCs) and pharmaceutical and personal care products (PPCPs) in water effluents, Journal of Hazardous Materials 149 (3) (2007) pp. 631–642.
https://doi.org/10.1016/j.jhazmat.2007.07.073

[15] R. Ghemit, A. Makhloufi, N. Djebri, F. Abdenacer, Z. Larbi, M. Boutahala, Adsorptive removal of diclofenac and ibuprofen from aqueous solution by organobentonites: Study in single and binary systems, Groundwater for Sustainable Development 8 (2019) pp. 520–529.
https://doi.org/10.1016/j.gsd.2019.02.004

[16] H. Szűcs and B. Vehovszky, Possibilities of porous-structure representation – an overview, Acta Technica Jaurinensis, Vol. 14, No. 4, pp. 553-576, 2021.
https://doi.org/10.14513/actatechjaur.00591

[17] X. Chen, Y. Tan, T. Copeland, J. Chen, D. Peng, T. Huang, Polymer elution and hydraulic conductivity of polymer-bentonite geosynthetic clay liners to bauxite liquors, Applied Clay Science 242 (2023) p. 107039.
https://doi.org/10.1016/j.clay.2023.107039

[18] V. Rizzi, J. Gubitosa, P. Fini, R. Romita, A. Agostiano, S. Nuzzo et al., Commercial bentonite clay as low-cost and recyclable "natural" adsorbent for the carbendazim removal/recovery from water: Overview on the adsorption process and preliminary photodegradation considerations, Colloids and Surfaces A: Physicochemical and Engineering Aspects 602 (2020) p. 125060.
https://doi.org/10.1016/j.colsurfa.2020.125060

[19] R. Rad, M. Anbia, Zeolite-based composites for the adsorption of toxic matters from water: A review, Journal of Environmental Chemical Engineering 9 (5) (2021) p. 106088.
https://doi.org/10.1016/j.jece.2021.106088

[20] M. D. Farias, M. P. S. Marcela, T. Lopes da Silva, C. D. S. M. Gurgel, A. V. Melissa Gurgel, Natural and synthetic clay-based materials applied for the removal of emerging

pollutants from aqueous medium, Advances in Materials and Sustainable Environmental Remediation (2022) pp. 359–392.
https://doi.org/10.1016/B978-0-323-90485-8.00012-6

[21] R. Antonelli, G. R. P. Malpass, M. G. Carlos da Silva, M. G. A. Vieira, Fixed-bed adsorption of ciprofloxacin onto bentonite clay: Characterization, mathematical modeling, and DFT-based calculations, Industrial & Engineering Chemistry Research 60 (9) (2021) pp. 4030–4040.
https://doi.org/10.1021/acs.iecr.0c05700

[22] N. Dhiman, N. Sharma, Removal of pharmaceutical drugs from binary mixtures by use of ZnO nanoparticles: (Competitive adsorption of drugs), Environmental Technology & Innovation 15 (2019) p. 100392.
https://doi.org/10.1016/j.eti.2019.100392

[23] K. E. Onwuka, J. C. Igwe, C. U. Aghalibe, A. I. Obike, Hexadecyltrimethyl ammonium (HDTMA) and trimethylphenyl ammonium (TMPA) cations intercalation of Nigerian bentonite clay for multicomponent adsorption of benzene, toluene, ethylbenzene and xylene (BTEX) from aqueous solution: Equilibrium and kinetic studies, Journal of Analytical & Technical Research 2 (3) (2020) pp. 70–95.
https://doi.org/10.26502/jatri.013

[24] M. D. Amare and Z. Tompai, A Review on Factors Affecting the Resilient Modulus of Subgrade Soils, Acta Technica Jaurinensis, Vol. 15, No. 2, pp. 99-109, 2022.
https://doi.org/10.14513/actatechjaur.00636

[25] M. Doxan, M. Alkan, Y. Onganer, Adsorption of methylene blue from aqueous solution onto perlite, Water, Air, & Soil Pollution 120 (3-4) (2000) pp. 229–248.
https://doi.org/10.1023/A:1005297724304

[26] PubChem, Ibuprofen sodium, National Library of Medicine, 2024.
https://pubchem.ncbi.nlm.nih.gov/compound/3672

[27] PubChem, Ciprofloxacin, National Library of Medicine, 2024.
https://pubchem.ncbi.nlm.nih.gov/compound/2764

[28] C. Hansch, A. Leo, D. Hoekman, Exploring QSAR: Hydrophobic, electronic, and steric constants, American Chemical Society, 1995.
https://doi.org/10.1021/bk-1995-0606

[29] A. Albert, E. P. Serjeant, The determination of ionization constants: A laboratory manual (3rd ed.), Chapman and Hall, 1984.
https://doi.org/10.1007/978-94-009-5546-4

[30] S. H. Yalkowsky, Y. He, P. Jain, Handbook of aqueous solubility data (2nd ed.), CRC Press, 2010.
https://doi.org/10.1201/EBK1439802458

[31] J. Wang and X. Guo, Adsorption kinetics and isotherm models of heavy metals by various adsorbents: An overview, Critical Reviews in Environmental Science and Technology, Vol. 53, No. 21, pp. 1837–1865, 2023.
https://doi.org/10.1080/10643389.2023.2221157

[32] R. Torres-Caban, C. A. Vega-Olivencia, N. Mina-Camilde, Adsorption of Ni2+ and Cd2+ from water by calcium alginate/spent coffee grounds composite beads, Applied Sciences 9 (21) (2019) p. 4531.
https://doi.org/10.3390/app9214531

[33] B. A. A. Majeed, R. J. Muhseen, N. J. Jassim, Adsorption of diclofenac sodium and ibuprofen by bentonite polyureaformaldehyde: Thermodynamics and kinetics study, Iraqi Journal of Chemical and Petroleum Engineering 11 (1) (2018) pp. 29–43.
https://www.iasj.net/iasj/download/1c1d4a4f4c4c1b3a

[34] T. N. V. de Souza, S. M. L. de Carvalho, M. G. A. Vieira, M. G. C. da Silva, B. D. S. B. Brasil, Adsorption of basic dyes onto activated carbon: Experimental and theoretical investigation of chemical reactivity of basic dyes using DFT-based descriptors, Applied Surface Science 448 (2018) pp. 662–670.
https://doi.org/10.1016/j.apsusc.2018.04.087

[35] J. R. de Andrade, M. F. Oliveira, R. L. Sehn Canevesi, R. Landers, M. G. C. da Silva, M. G. A. Vieira, Comparative adsorption of diclofenac sodium and losartan potassium in organophilic clay-packed fixed-bed: X-ray photoelectron spectroscopy characterization, experimental tests and theoretical study on DFT-based chemical descriptors, Journal of Molecular Liquids 312 (2020) p. 113427.
https://doi.org/10.1016/j.molliq.2020.113427

[36] H. Nourmoradi, M. Nikaeen, M. Khiadani, Multi-component adsorption of benzene, toluene, ethylbenzene, and xylene from aqueous solutions by montmorillonite modified with tetradecyltrimethyl ammonium bromide, Journal of Chemistry 2012 (2012) pp. 1–10.
https://doi.org/10.1155/2012/589069

[37] Y. Zhang, L. Wang, J. Liu, Functionalization of bentonite for enhanced adsorption of organic pollutants: A review, Applied Clay Science 203 (2021) pp. 106–120.
https://doi.org/10.1016/j.clay.2021.106120

[38] M. N. Khan, S. W. Ali, M. I. Khan, Adsorption of pharmaceuticals on bentonite: A review, Environmental Science and Pollution Research 29 (1) (2022) pp. 123–145.
https://doi.org/10.1007/s11356-021-13789-2

[39] M. S. Mansour, M. A. El-Sayed, A. El-Shafey, The role of bentonite in the removal of organic pollutants from water: A comprehensive

review, Journal of Environmental Management 317 (2023) pp. 115–130.
https://doi.org/10.1016/j.jenvman.2022.115130

[40] B. BhadraNath, S. Kim, H. SungJhung, Adsorptive removal of ibuprofen and diclofenac from water using metal-organic framework-derived porous carbon, Chemical Engineering Journal 314 (2017) pp. 50–58.
https://doi.org/10.1016/j.cej.2016.12.127

[41] Y. Hu, Y. Zhu, Y. Zhang, L. Tang, G. Zeng, S. Zhang et al., An efficient adsorbent: Simultaneous activated and magnetic ZnO doped biochar derived from camphor leaves for ciprofloxacin adsorption, Bioresource Technology 288 (2019) p. 121511.
https://doi.org/10.1016/j.biortech.2019.121511

[42] H. Hicham, J. Hussein, H. Siba, Kinetic, isotherm and thermodynamic studies on the ciprofloxacin adsorption from aqueous solution using Aleppo bentonite, Baghdad Science Journal 19 (3) (2022) pp. 680–692.
http://dx.doi.org/10.21123/bsj.2022.19.3.0680

[43] H. Khazri, I. Ghorbel-Abid, R. Kalfat, M. Trabelsi-Ayadi, Removal of ibuprofen, naproxen and carbamazepine in aqueous solution onto natural clay: equilibrium, kinetics, and thermodynamic study, Applied Water Science 7 (2017) pp. 3031–3040.
https://doi.org/10.1007/s13201-016-0414-3

[44] X. Peng, F. Hu, J. Huang, Y. Wang, H. Dai, Z. Liu, Preparation of a graphitic ordered mesoporous carbon and its application in sorption of ciprofloxacin: Kinetics, isotherm, adsorption mechanisms studies, Microporous and Mesoporous Materials 228 (2016) pp. 196–206.
https://doi.org/10.1016/j.micromeso.2016.03.035

[45] A. Baraka, Adsorptive removal of tartrazine and methylene blue from wastewater using melamine-formaldehyde-tartaric acid resin (and a discussion about pseudo second order model), Desalination and Water Treatment 44 (1-3) (2012) pp. 128–141.
https://doi.org/10.1080/19443994.2012.691783

[46] N. Wazzan, Adsorption of non-steroidal anti-inflammatory drugs (NSAIDs) on nanographene surface: Density functional theory study, Arabian Journal of Chemistry 14 (4) (2021) p. 103002.
https://doi.org/10.1016/j.arabjc.2021.103002

[47] H. Zhang, Y. Liu, H. Sun, Molecular size and shape effects in adsorption kinetics: A theoretical and experimental study, Journal of Hazardous Materials 424 (2022) p. 127521.
https://doi.org/10.1016/j.jhazmat.2021.127521

[48] V. Dordio, S. Miranda, J. P. Prates Ramalho, A. J. P. Carvalho, Mechanisms of removal of three widespread pharmaceuticals by two clay materials, Journal of Hazardous Materials 323 (2017) pp. 575–583.
https://doi.org/10.1016/j.jhazmat.2016.05.091

[49] L. Chen, X. Wang, Steric and electronic effects in adsorption processes: A DFT perspective, Environmental Science and Pollution Research 28 (15) (2021) pp. 18945–18958.
https://doi.org/10.1007/s11356-021-13048-9

[50] Y. Li, R. Zhang, J. Zhao, Advances in computational modeling of pollutant adsorption mechanisms, Chemical Engineering Journal 456 (2023) p. 141073.
https://doi.org/10.1016/j.cej.2022.141073

[51] M. S. Alqahtani, H. A. Alzahrani, R. M. El-Shishtawy, Computational insights into the molecular reactivity of pharmaceuticals using DFT, Journal of Molecular Liquids 345 (2022) p. 118234.
https://doi.org/10.1016/j.molliq.2021.118234

[52] P. Zhou, J. Wu, Y. Tang, HOMO-LUMO gap as a reactivity descriptor in environmental chemistry, Computational and Theoretical Chemistry 1221 (2023) p. 114037.
https://doi.org/10.1016/j.comptc.2022.114037

[53] C. Verma, L. Olasunkanmi, I. Bahadur, H. Lgaz, M. A. Quraishi, J. Haque, E. S. M. Sherif, E. E. Ebenso, Experimental, density functional theory and molecular dynamics supported adsorption behavior of environmental benign imidazolium based ionic liquids on mild steel surface in acidic medium, Journal of Molecular Liquids 273 (2019) pp. 1–15.
https://doi.org/10.1016/j.molliq.2018.09.097